Dislocation Pinning by Small Interstitial Loops: A Molecular Dynamics Study

D. Rodney and G. Martin
Section de Recherches de Métallurgie Physique, CEA/Saclay, 91191 Gif-sur-Yvette, France
(Received 30 November 1998)

Molecular dynamics simulations show that, in an embedded atom method nickel crystal, interstitial loops with appropriate geometries, made of four ⟨110⟩ dumbbells, are absorbed by the Shockley partials of both static and gliding edge dislocations. Depending on the applied stress, the loops may be either dragged and undergo atomic-level rearrangements or unpin from the dislocation. Such loops induce an additional friction for the dislocation glide which is evaluated from the simulations. Similar effects are also observed when loops with different geometries stabilize a few lattice planes away from the dislocation glide plane. [S0031-9007(99)08918-8]

PACS numbers: 61.72.Bb

Irradiation induced hardening of metals and alloys is known experimentally since the early 1950s [1] but the hardening mechanisms are still open to discussion. Two main mechanisms have been proposed: the *dispersed barrier hardening* [2], on the one hand, where irradiation defects (vacancy or interstitial clusters) act as barriers to the motion of the dislocations and the *source hardening* [3], on the other hand, where dislocation sources are locked in by defect clouds. Extensive calculations of dislocation/defect interactions were carried out in the 1960s and 1970s (e.g., [4]) but mainly dealt with long-range forces since they were based on elasticity theory.

In the last decade, the renewal of molecular dynamics (MD) simulations of displacement cascades gave new insights on defect clustering. In face-centered-cubic (fcc) metals, small dislocation loops that are made of less than 20 ⟨110⟩ dumbbell interstitials, were found to form at the periphery of the cascades [5,6]. Similar small glissile loops also form in simulations of bcc iron and $L1_2$ Ni_3Al [7]. These loops are highly mobile in one dimension, along their glide cylinder. Recently, Trinkaus, Singh, and Foreman [8] proposed that such dumbbell clusters could play a major role in source hardening since they can glide over large distances and be trapped in the strain field of dislocations, resulting in the formation of defect clouds. However, the above analysis was based on elasticity theory. Moreover, the direct observation in transmission electron microscopy (TEM) of the one-dimensional glide of interstitial loops and their agglomeration in the vicinity of edge dislocations have only been possible for loops of radii greater than 1 nm [9], because of the TEM resolution.

Following the pionnering work of Daw *et al.* [10,11] and in view of the recent advances in the MD simulations of dislocation dynamics [12,13], we have undertaken an atomistic study of dislocation pinning by small interstitial loops. We report here the first results concerning the interactions between an interstitial loop made of four ⟨110⟩ dumbbells, and both static and gliding edge dislocations in a fcc nickel crystal. Our aim is to characterize atomic-level reactions and evaluate the effect of the cluster on the dislocation mobility.

The main characteristics of the simulations are as follows. The embedded atom method potential developed by Angelo *et al.* [14] is used to simulate a nickel crystal. The simulation cell is sketched in Fig. 1. Its dimensions are 20 nm × 17 nm × 6 nm in directions X, Y, and Z, respectively, and it contains 200 000 atoms. An edge $a/2[110](1\bar{1}1)$ dislocation is inserted by virtue of its elastic displacement field along the central $Y = [\bar{1}12]$ atomic row of the cell. A conjugate gradient energy minimization allows the dislocation to dissociate in the $(1\bar{1}1)$ plane at $Z = 0$ into two Shockley partials with Burgers vectors $\mathbf{A}\beta$ and $\beta\mathbf{C}$. The following boundary conditions, adapted from those used by Daw *et al.* [10,11], turned out to be very effective. Periodic boundary conditions are used in the $X = [110]$ and $Y = [\bar{1}12]$ directions: an array of infinite parallel dislocations is thus simulated. In the $Z = [1\bar{1}1]$ direction, the atoms lying in the upper and lower $(1\bar{1}1)$ surfaces are constrained to two-dimensional dynamics: they are fixed in the Z direction. Similar conditions were used recently in static simulations [15] and allow for atomic relaxations inside the $(1\bar{1}1)$ surfaces both

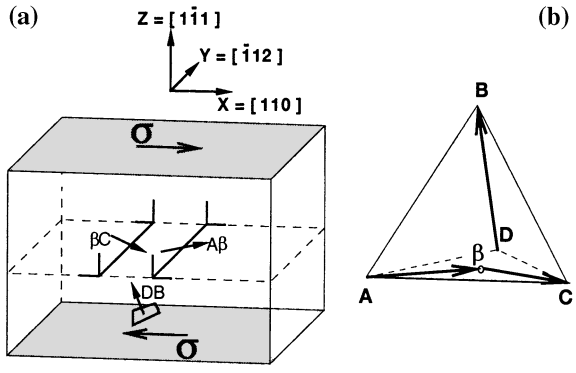

FIG. 1. Schematic view of the simulation cell (a) and corresponding Thompson tetrahedron (b). The origin of the coordinate system is taken at the center of the cell.

 0031-9007/99/82(16)/3272(4)$15.00 © 1999 The American Physical Society

when the dislocation is at rest and when it moves in its glide plane.

A shear stress σ_{xz} may be applied by superimposing constant forces in the [110] direction to the forces felt by the atoms in the $(1\bar{1}1)$ surfaces, as shown in Fig. 1(a). The forces in the upper and lower surfaces have opposite directions and the upper force is scaled to account for the two extra half planes introduced by the edge dislocation. The stress σ_{xz} ranges from 7.5 to 300 Mpa which corresponds to stresses from 0.006% to 0.24% of C_{44}, the shear modulus (125 GPa).

We consider the interactions between the dislocation described above and a four-interstitial cluster. The interstitials are inserted *by hand* in the crystal between two {111} planes. In the case of the cluster shown in Fig. 1(a), the interstitials are inserted between two $(1\bar{1}1)$ planes. In the absence of the dislocation, as discussed in Ref. [6], the configuration of lower energy for such a cluster consists of dumbbells centered around a single $(1\bar{1}1)$ plane and aligned in a same $\langle 110 \rangle$ direction which, in the present case, is the **BD** direction of Fig. 1(b). At finite temperature, the cluster glides erratically along this direction. The **BD** vector is the Burgers vector of the cluster when the latter is considered as a small dislocation loop.

In presence of the *static* edge dislocation, the loop may either be absorbed by one of the Shockley partials or may stabilize away from the dislocation. We discuss first the case of absorption and focus on the configuration of Fig. 1 where the reaction is assisted by a change of the Burgers vector of the defect cluster. The interstitials are initially placed 1 nm below the stacking fault ribbon of the dislocation. In the course of an energy minimization, they first relax to form the four **BD** dumbbells expected in the absence of the dislocation. Upon further minimization, the loop starts to glide along its Burgers vector towards the dislocation and stops when it reaches the plane just below the stacking fault ribbon. The system is then in an energy minimum and the loop cannot glide any further since its glide cylinder intersects the plane of the stacking fault.

The loop is absorbed when thermal vibrations are allowed: a fixed temperature is imposed by periodically rescaling the atomic velocities [16]. At 100 K, the defect transforms within 1 ps into a new loop with both a new plane, parallel to the *BCD* plane of Fig. 1(b), and a new Burgers vector equal to the **AD** vector. Two of the four dumbbells are now in the $(1\bar{1}1)$ plane of the stacking fault while the other two are in the plane just below. The loop then glides along its new Burgers vector towards the $\mathbf{A}\beta$ partial dislocation and is absorbed in the core of this dislocation as shown in Fig. 2. This figure presents the region of the stacking fault plane of the dislocation near the loop. The cores of the partial dislocations, defined as regions where the local atomic order is neither fcc nor hcp, are shown in black. The attraction of the **AD** loop to the $\mathbf{A}\beta$ partial, rather than to the $\beta\mathbf{C}$ partial, can be

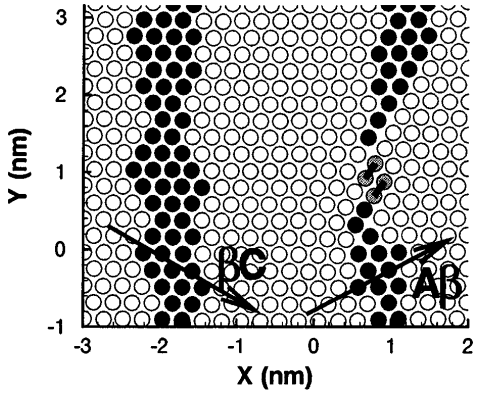

FIG. 2. Portion of the dislocation glide plane. Atoms in black belong to the cores of the $\mathbf{A}\beta$ and $\beta\mathbf{C}$ partials. Two dumbbells appear in grey.

rationalized by the fact that the loop and the partial locally form a $\mathbf{DA} + \mathbf{A}\beta = \mathbf{D}\beta$ junction which is energetically favorable according to Frank's rule [17].

The binding energy of the cluster to the dislocation is defined as the balance between, on the one hand, the sum of the energies of the present configuration plus that of the defect free cell, and, on the other hand, the sum of the energies of the cell with the dislocation alone plus that with the cluster alone placed at a reference position. The binding energy thus found is high: 6 eV, i.e., 1.5 eV per dumbbell. It is independent of the cell dimensions and of the reference position of the cluster as long as the latter is not too close to the $(1\bar{1}1)$ surfaces. The magnitude of the binding energy implies that the cluster cannot escape by thermal activation. By varying the initial distance between the loop and the dislocation, the maximum capture distance below the dislocation was estimated to be 3.5 nm at 100 K and only 1.8 nm at 0 K. A study of this temperature dependence is underway and will be discussed in Ref. [18].

The loop may also be absorbed by a *gliding* dislocation. This point is made clear by placing a **BD** loop ahead of the dislocation, 2 nm either above or below its glide plane. The dislocation is set in motion by applying, at 100 K, a stress $\sigma = 30$ Mpa. When the dislocation approaches, the loop is gradually attracted to the glide plane in agreement with elastic calculations [4]. The defect is then *hit* by the front partial and absorbed in the core of this dislocation resulting in the same configuration as the static one. Therefore, a gliding dislocation absorbs irradiation defects that lie near its glide plane. This *sweeping* mechanism certainly contributes to the formation of the *clear bands* observed experimentally in deformed irradiated materials [4,19]: in such materials, the deformation is localized along slip bands which, after deformation, are nearly clear of any irradiation defect.

We now consider the response of the dislocation containing a cluster to an applied shear stress. The initial configuration is the static configuration considered above maintained at 100 K. At time $t = 0$ ps, a low stress

(30 Mpa) is applied and the dislocation gradually accelerates to reach a terminal steady velocity, dragging along the loop in much the same way as a classical jog [20]. The loop glides along its **AD** Burgers vector at 60° from the glide direction of the dislocation. The partial containing the loop bows out between the defect and its periodic images, with a curvature increasing with stress. The second partial remains almost straight. If a higher stress is applied (150 Mpa), an atomic-level reaction is observed. Figure 3 shows the configuration of the dislocation before, during, and after the transformation. During the initial acceleration phase [Fig. 3(a)], the loop is dragged in the **AD** direction as in the previous case. The distance between the loop and the back partial gradually decreases until this dislocation is in contact with the defect cluster, resulting in a constriction of the dissociated dislocation [Fig. 3(b)]. This configuration is unstable and the front partial breaks away leaving the loop inside the core of the back partial. The loop remains attached to the back partial and rearranges to adopt a new Burgers vector, the **AC** vector parallel to the glide direction [Fig. 3(c)]. It is then dragged in this direction by the dislocation which reaches a steady velocity. The binding energy is 5.3 eV, therefore lower than before the change of the Burgers vector.

At still higher stresses (300 Mpa), unpinning is observed but only as a transient state: because of the periodic boundary conditions, the dislocation comes back onto the cluster and interacts again with it. The dumbbells remain then attached to the back partial with the same configuration as in Fig. 3(c).

We now discuss the dislocation terminal velocity as a function of the applied stress σ, as shown in Fig. 4. In the absence of defect clusters (the dashed curve) and at low stresses ($\sigma < 30$ Mpa), the free dislocation velocity is proportional to the applied stress in agreement with dislocation drag theory [21]: the dissipation of the deformation field of the dislocation in the phonon gas of the crystal induces a viscous friction on the dislocation that limits its velocity. The friction coefficient, calculated from the initial slope of the free velocity at 100 K, is $\nu_0 = \sigma b/v = 5 \times 10^{-6}$ Pa s which is a lower limit for experimental friction coefficients [21].

At high stresses, the velocity saturates at 2.1 nm ps^{-1}, i.e., 72% of the transverse sound wave velocity (2.9 nm ps^{-1}), independently of the temperature in the range 10 to 100 K, and of the cell dimensions. It compares well with that found by Daw *et al.* [11].

The defect clusters increase the friction on the dislocation up to $\nu = 8 \times 10^{-6}$ Pa s at low stresses and 100 K. Figure 4 shows that below the threshold stress of 110 Mpa, the steady velocity increases with stress and saturates at 0.9 nm ps^{-1}, independently of the temperature. Since the loop has a Burgers vector at 60° from that of the dislocation, it travels twice as fast as the dislocation. Its velocity reaches 1.8 nm ps^{-1} which is the highest velocity reached by a loop in all our simulations. The plateau may therefore be explained by a relativistic saturation of the loop velocity, as considered in the case of jog drag [20]: the defect cluster has reached its maximum velocity and limits the velocity of the dislocation. Beyond the threshold stress, the loop rearranges as described above and glides in the same direction as the dislocation and therefore at the same velocity. The dislocation velocity is no longer limited to 0.9 nm ps^{-1}, and, as seen in Fig. 4, jumps to 1.6 nm ps^{-1}. This velocity is lower than the free velocity which implies that the **AC** loop is also a source of additional friction for the dislocation glide.

The influence of the loop density along the dislocation line (b/l) was studied by using a simulation cell shorter in the Y direction ($l = 8.5$ nm instead of $l = 17$ nm). Details of the calculations will be given elsewhere [18]. Briefly, we found, as shown in Fig. 5, that the velocity of the dislocation is a function of σbl, the total force applied between two clusters, rather than a function of σ.

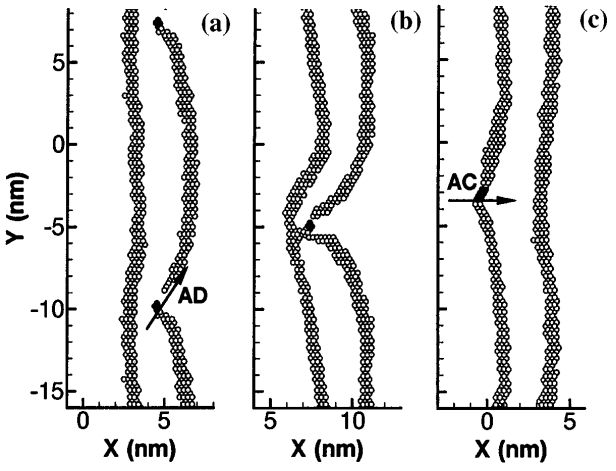

FIG. 3. Snapshots of the dislocation at $\sigma = 150$ Mpa, $T = 100$ K, and after, respectively, 3 ps (a), 9 ps (b), and 15 ps (c). The dumbbells appear in black. The vectors indicate the Burgers vector of the loop. The figure includes part of the periodic image of the dislocation.

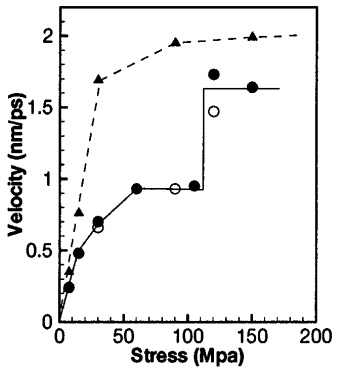

FIG. 4. Dislocation velocity as a function of applied stress. The dashed curve corresponds to the free dislocation. Empty symbols were obtained at $T = 10$ K; full symbols, $T = 100$ K.

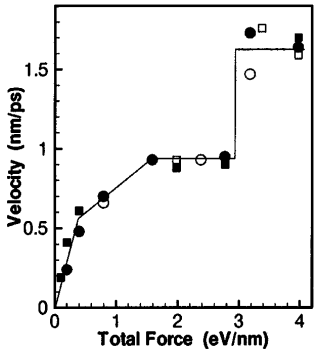

FIG. 5. Scaling of the dislocation velocity with the force σbl. Squares correspond to $l = 8.5$ nm, circles to $l = 17$ nm, empty symbols to $T = 10$ K, full symbols to $T = 100$ K.

Moreover, it appears that the Burgers vector change occurs at a critical applied force (equal to 3 eV nm^{-1}), as is the case for static unpinning [11].

We also investigated the case when the loop comes to a stable position away from the glide plane. We placed an **AD** loop ahead of the dislocation, 1 nm below its glide plane. With the **AD** vector being in a plane parallel to the glide plane, the loop cannot reach the dislocation by simple glide. Upon initial energy minimization, the defect cluster comes to a stable position under the $\mathbf{A}\beta$ partial, in agreement with simple elastic calculations. The binding energy is 2.3 eV, therefore lower than in the previous cases, but still high enough to impede a thermally activated escape. This configuration is stable up to 100 K and no Burgers vector change is observed.

When a low stress (30 Mpa) is applied at 100 K, the loop, gliding along its own Burgers vector, is dragged by the $\mathbf{A}\beta$ partial. The dislocation reaches a terminal velocity 40% below its free velocity. At higher stresses (150 Mpa), the dislocation breaks away within 10 ps. When it is back above the loop, hardly any interaction is seen and the dislocation reaches a terminal velocity equal to its free velocity. Therefore even when the small loop is as close as 1 nm from the glide plane, it offers no resistance to the fast dislocation.

The simulations presented here show that when a dislocation glides at low velocity in the vicinity of a small interstitial loop, the latter, independently of its Burgers vector, is captured by the dislocation and may be dragged over large distances. A systematic study of this sweeping mechanism is underway, in which we consider jogged dislocations and a broader variety of clusters, including larger interstitial clusters and vacancy clusters.

The authors thank Dr. N. V. Doan for his help in the MD simulations. Many helpful and insightful discussions with Pr. Y. Bréchet and Dr. C. Robertson are gratefully acknowledged.

[1] A. W. McReynolds, W. Augustiniak, M. McKewon, and D. B. Rosenblatt, Phys. Rev. **98**, 418 (1955).
[2] A. Seeger, in *Proceedings of the 2nd UN International Conference on Peaceful Uses of Atomic Energy* (United Nations, Geneva, 1958), Vol. 6, p. 250.
[3] T. H. Blewitt, R. R. Coltman, R. E. Jamison, and J. K. Redman, J. Nucl. Mater. **2**, 277 (1960).
[4] M. J. Makin, Philos. Mag. **10**, 695 (1964).
[5] T. Diaz de la Rubia and M. W. Guinan, Phys. Rev. Lett. **66**, 2766 (1991).
[6] A. J. E. Foreman, C. A. English, and W. J. Phythian, Philos. Mag. A **66**, 655 (1992); A. J. E. Foreman, W. J. Phythian, and C. A. English, Philos. Mag. A **66**, 671 (1992).
[7] N. V. Doan and R. Vascon, Nucl. Instrum. Methods Phys. Res., Sect. B **135**, 207 (1998).
[8] H. Trinkaus, B. N. Singh, and A. J. E. Foreman, J. Nucl. Mater. **249**, 91 (1997); B. N. Singh, A. J. E. Foreman, and H. Trinkaus, J. Nucl. Mater. **249**, 103 (1997).
[9] M. Kiritani, J. Nucl. Mater. **251**, 237 (1997).
[10] M. S. Daw, M. I. Baskes, C. L. Bisson, and W. G. Wolfer, in *Modeling Environmental Effects on Crack Growth Processes*, edited by R. H. Jones and W. W. Gerberich (The Metallugical Society, Warrendale, PA, 1986), p. 99.
[11] M. S. Daw, S. M. Foiles, and M. I. Baskes, Mater. Sci. Rep. **9**, 251 (1993).
[12] V. Bulatov, F. Abraham, L. Kubin, B. Devincre, and S. Yip, Nature (London) **391**, 669 (1998).
[13] S. J. Zhou, D. L. Preston, P. S. Lomdahl, and D. M. Beazley, Science **279**, 1525 (1998).
[14] J. E. Angelo, N. R. Moody, and M. I. Baskes, Model. Simul. Mater. Sci. Eng. **3**, 289 (1995).
[15] A. Aslanides and V. Pontikis, Comput. Mater. Sci. **10**, 401 (1998).
[16] M. P. Allen and D. J. Tildesley, *Computer Simulation of Liquids* (Clarendon Press, Oxford, England, 1987), p. 228.
[17] F. C. Frank, Physica (Utrecht) **15**, 131 (1949).
[18] D. Rodney and G. Martin (to be published).
[19] I. G. Greenfield and H. G. F. Wilsdorf, J. Appl. Phys. **32**, 827 (1961).
[20] J. Friedel, *Dislocations* (Pergamon Press, Oxford, 1964).
[21] V. I. Alshits and V. L. Indenbom, in *Dislocations in Solids*, edited by F. R. N. Nabarro (North-Holland, Amsterdam, 1986), Vol. 7, p. 43.